ELSEVIER

Journal of Nuclear Materials 241–243 (1997) 426–432

journal of nuclear materials

Parallel electron temperature and density gradients measured in the JET MkI divertor using thermal helium beams

S.J. Davies [a,*], P.D. Morgan [a], Y. Ul'Haq [a,b], C.F. Maggi [a], S.K. Erents [a,c], W. Fundamenski [a,d], L.D. Horton [a], A. Loarte [a], G.F. Matthews [a], R.D. Monk [a], P.C. Stangeby [a,d]

[a] *JET Joint Undertaking, Abingdon, Oxon OX14 3EA, UK*
[b] *Imperial College of Science, Technology and Medicine, London SW7 2BZ, UK*
[c] *UKAEA Fusion, Culham, Abingdon, Oxon OX14 3EA, UK*
[d] *Institute for Aerospace studies, University of Toronto, Toronto, Canada*

Abstract

This paper describes the first application of a thermal helium beam diagnostic to a divertor. The helium beam is used to determine spectroscopically the electron temperature and density from the inner and outer strike points up to the X-point, using helium line ratios which are primarily sensitive to electron density and temperature, as reported by Schweer et al. [J. Nucl. Mater. 196–198 (1992) 174]. Measurement of the neutral helium line intensities in the outer divertor target were performed under attached, high recycling and detached plasma conditions in Ohmic and L-mode discharges. An interpretative model has been developed using the DIVIMP code at JET which incorporates the helium injection point, the nozzle divergence and the viewing arrangement of the periscope for a particular equilibrium.

Keywords: Divertor plasma; Monte Carlo simulation; Detached plasma; Plasma density and temperature diagnostic; Atomic physics

1. Introduction

Measurement of the distribution of electron temperature and density from the inner and outer strike points up to and beyond the X-point are basic parameters crucial for the understanding of divertor physics. For example such information can be used to identify where a particular impurity will radiate the most. These parameters are also needed in the validation of detachment models like, for example, EDGE2D [2]. In this paper the first application of a thermal helium beam diagnostic to a divertor, capable of providing simultaneous measurements of the 2D distribution of electron density and temperature from the inner and outer strike points up to the X-point, is described. Neutral helium line ratios which are primarily sensitive to electron density (667.82 nm/728.13 nm) and temperature (706.52 nm/728.13 nm) as reported in Ref. [1] are used. Data presented concentrate on measurements performed in the outer divertor leg for Ohmic and L-mode diverted discharges at various stages of detachment. Target electron densities and temperatures are provided from Langmuir probe measurements which may, under high recycling and detached conditions, overestimate the electron temperature, as the sheath resistance begins to have a dominant effect upon the IV characteristic and a virtual double probe fitting routine has to be employed. Further details on this subject are given in Ref. [3].

The development of an interpretative model using the divertor impurity code DIVIMP [4] which generates the background hydrogenic plasma and incorporates diagnostic lines-of-sight utilizing the JET atomic database ADAS [5] is also described. Such a model makes it easier to integrate experimental data with the modelling of detachment.

* Corresponding author. Tel.: +44-1235 528 822; fax: +44-1235 464 766; e-mail: sdavies@jet.uk.

PII S0022-3115(96)00541-7

2. Experimental arrangement

The arrangement of the helium injection nozzle and periscope for measurements in the outer divertor leg is shown in Fig. 1. Target Langmuir probes were also situated in the same octant. Helium was injected at a rate of 13 mbar l/s ($\sim 3 \times 10^{20}$ He atoms/s) for typically two seconds with a thermal velocity of $\sim 2 \times 10^3$ m/s and the 'nozzle' used within the divertor was a 2 mm ID 45 mm long pipe with backing pressure ~ 200 mbar. This was expected to give a divergence of $\sim 40°$ FWHM [6]. The measurement of this divergence is currently being undertaken at IPP Berlin.

The periscope consisted of ten 300 μm all-silica fibres which covered a vertical distance of 60 cm from the divertor floor. The fibres have a numerical aperture of 0.2 giving a 2.5 cm diameter viewing cone at the helium injection point. A Spex 270 M spectrometer with CCD camera, having a resolution of 0.13 nm/pixel over a spectral range of 100 nm at a 100 ms sampling rate, was used to record the spectral intensities, an example of which is shown in Fig. 2a. The background level of helium in the results shown here was negligible. If a large background level exists then it is possible to modulate at, up to 2 Hz, the gas flow and to deconvolve the injected helium signal from the background recycling helium signal. Using a spectrometer to record simultaneously the neutral helium line intensities has certain advantages over using three independent CCD cameras with interference filters in that any time variations in sensitivities are reduced once a calibration has been done. In addition, it is possible to account for the different background levels at each wavelength rather than assume a constant level.

Once the background level has been subtracted from each HeI line intensity, the two ratios are calculated and an example is shown in Fig. 2b. Note that before the establishment of the helium flow from 13 s onwards the fluctuation level in the ratios is large as a result of taking ratios of two small numbers. The HeI line intensities before this time are comparable to the background continuum level. This noise level reduces significantly after 13 s when the HeI line intensities become significantly higher than the background until after 19 s, when the helium injection has stopped and hence the HeI line intensities have decreased, when the fluctuation level begins to increase again. Electron densities and temperatures are calculated from these ratios using the atomic data and look up tables from the collisional–radiative model of [7]. In the future this step will be automated through collaboration with B. Schweer et al. at TEXTOR, KfA Jülich.

3. Experimental results

The neutral helium was injected from the private plasma region towards the separatrix where it was rapidly ionized. DIVIMP modelling of the neutral helium transport (of which more later) has shown that the photon emission at the wavelengths used is mainly from the separatrix. Consequently, thermal helium beam derived electron temperatures and densities given for the Ohmic and L-mode examples below are quoted as the separatrix values. The strike points were swept at 4 Hz and this sweeping is superimposed on the parallel electron density and temperature profiles shown below.

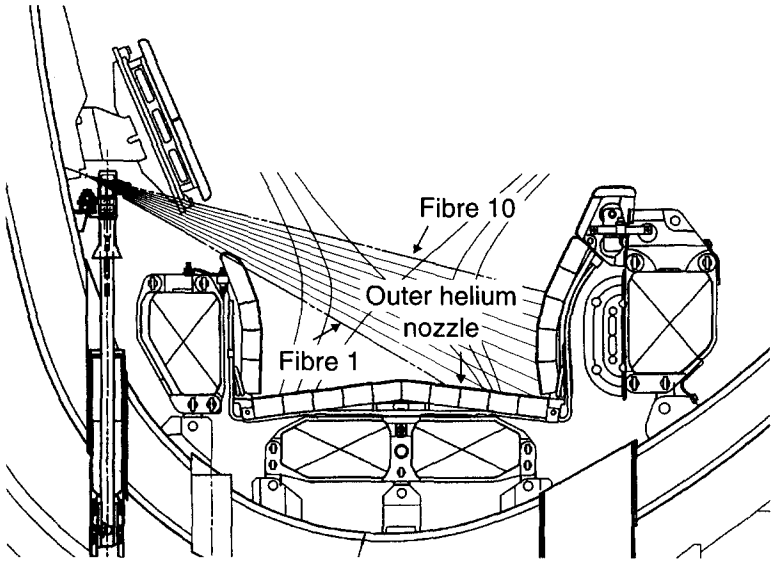

Fig. 1. Viewing arrangement for the thermal helium beam diagnostic in the JET MkI outer divertor leg with representative equilibria.

3.1. Ohmic density ramp pulse 35430

During this Ohmic pulse the central line-averaged density was ramped from 2 to 6×10^{19} m^{-3} and the onset of high recycling, at which the ion-flux to the inner and outer target began to decrease, occurred at a central density of 3.5×10^{19} m^{-3}. The inner target then became detached, Langmuir probe measurements giving a target electron temperature of 5 eV and density of $\sim 10^{18}$ m^{-3}, whilst the outer target became partially detached. Fig. 3 shows the evolution of the electron temperature and density from the outer target, measured by Langmuir probes, up to the X-point as measured by the thermal helium beam diagnostic. The upstream electron temperature is first seen to be higher than, then reduces to become comparable to, the target temperature which is suggestive of a 'detachment front' propagating up to the X-point, consistent with bolometer measurements on similar detached pulses [8].

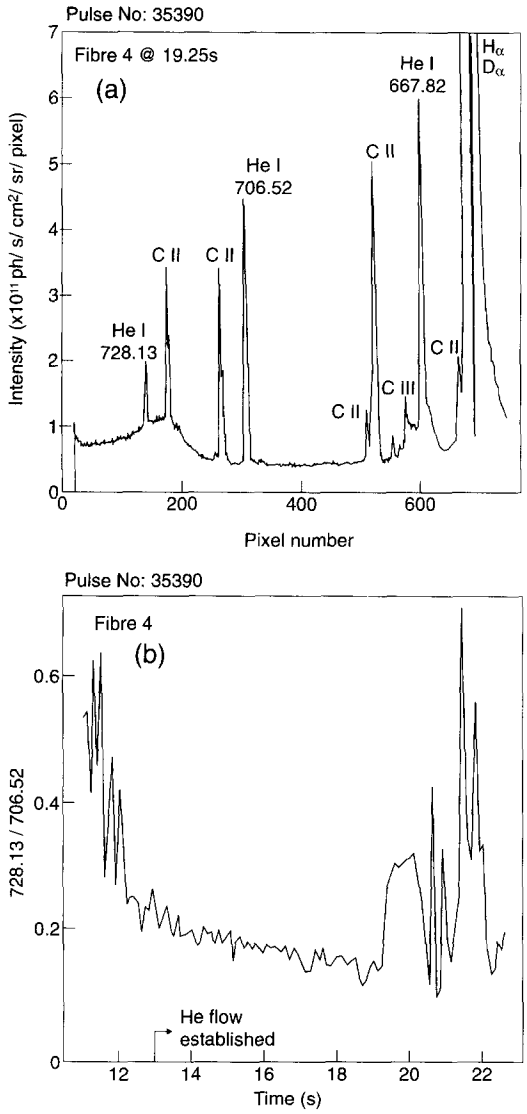

Fig. 2. (a) Example spectra recorded using Fibre 4 in Outer viewing periscope during L-mode pulse 35390 and (b) resulting evolution of helium line ratio 728.13 nm/706.52 nm.

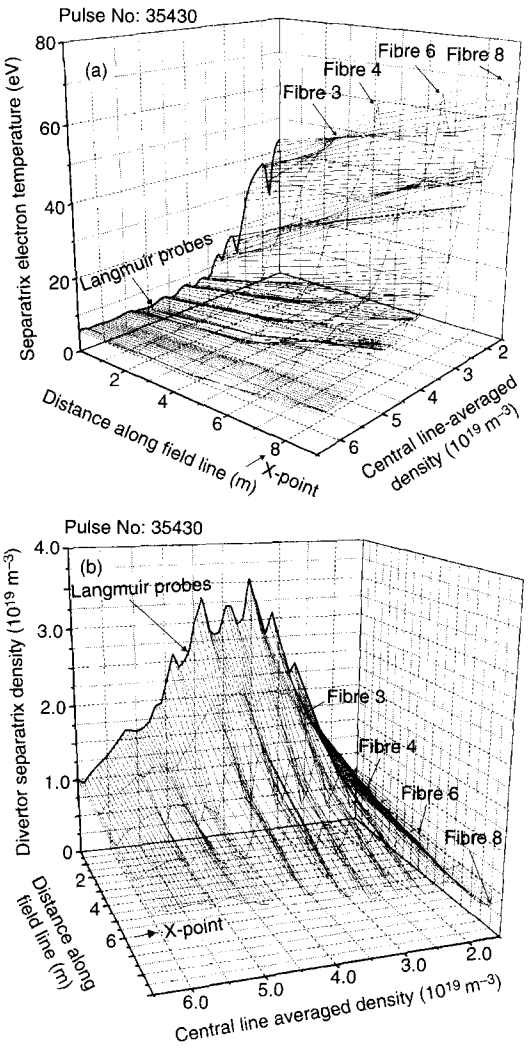

Fig. 3. Spatial variation of (a) electron temperature and (b) electron density in outer divertor leg as a function of line-averaged density for ohmic pulse 35430. Note that these profiles incorporate target Langmuir probe data and HeI line ratio data from fibers 3, 4, 6 and 8 with linear interpolation between these points.

The expected upstream temperatures calculated using the two-point model [9] were compared with those determined from the helium beam data and it was found that before the onset of detachment the agreement between the calculated and measured electron temperatures was generally good. With high recycling leading to detachment the two-point model calculations become invalid as no account is taken of parallel momentum losses through charge ex-

change. Consequently, a large difference between the expected and observed temperatures occurred that was first seen at 2.2 m along the field line and then further up towards the X-point.

Better agreement between modelled and measured electron temperatures was obtained with EDGE2D modelling [10] of the detachment as indicated in Table 1.

3.2. L-mode detachment pulse 35390

In this 3.8 MW neutral beam injected pulse the density was increased to 4.8×10^{19} m^{-3} at 13 s after which it remained constant up to 19 s. Neutral helium was injected over this time period and the resulting parallel electron density and temperature variation is illustrated as a function of time in Fig. 4. As previously the target electron densities and temperatures are provided from Langmuir probe measurements. The influence that the 4 Hz sweeping of the strike points has on the profiles is more clearly seen in this figure.

The temperature at the target decreased from 30 eV at 13 s to 7 eV at 15 s whilst at the X-point it decreased from 40 eV to 17 eV. The target density peaked at approximately 1×10^{20} m^{-3} whilst at the X-point it increased from 0.87×10^{19} m^{-3} to 1.5×10^{19} m^{-3}. Such a high divertor density means that other atomic processes, such as volume recombination, must be occurring. These are not taken into account in the collisional–radiative model of [7] and consequently the helium derived densities are probably lower than the actual densities. At the inner divertor target the electron temperature peaked at 20 eV at 13 s rapidly decreasing to 5 eV from 14 s onwards when the inner divertor leg became detached. Correspondingly the electron density peaked at 1.5×10^{20} m^{-3} reducing to $\leq 5 \times 10^{19}$ m^{-3}.

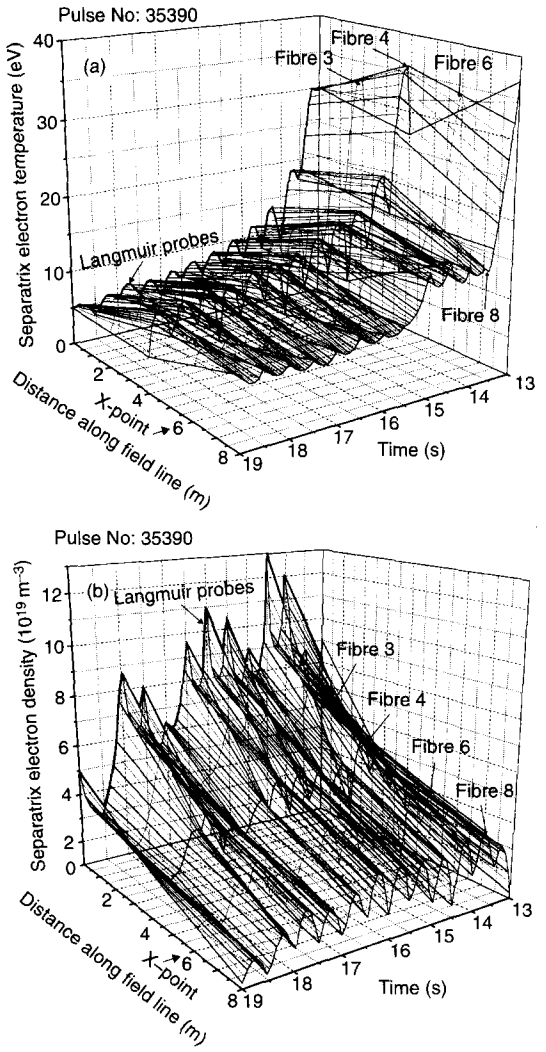

Fig. 4. Spatial variation of (a) electron temperature and (b) electron density in outer divertor leg as a function of time in pulse 35390. Note that these profiles incorporate target Langmuir probe data and HeI line ratio data from fibres 3, 4, 6 and 8 with linear interpolation between these points.

4. Development of an interpretative model using DIVIMP

The injection of helium atoms into the MkI divertor plasma and the measurement of neutral helium line intensities of 706.52 nm, 728.13 nm and 667.82 nm along diagnostic lines of sight have been simulated using DIVIMP, a Monte Carlo impurity transport code [4]. Helium atoms are launched into a background hydrogenic plasma from a point source and the trajectory of each particle is calculated using the Monte Carlo method. Toroidal sym-

Table 1
Comparison of EDGE2D calculated and measured electron temperatures at different distances along the outer divertor leg in Ohmic pulse 35430

Outer divertor conditions	EDGE2D (measured) upstream T_e (eV) at		
	2.2 m along field line	4.1 m along field line	8.1 m along field line
Low recycling	30(25)	35(30)	39(40)
High recycling	10(8.5)	14(15)	26(25)
Partial detachment	3(4.5)	5.5(6)	11(15)

metry is assumed and the particle motion is mapped onto a 2D poloidal plane. The calculations for both the background plasma and the injected impurities are performed on a non-orthogonal grid generated from magnetic measurements for a specific time in a pulse.

4.1. Background plasma

A 2D hydrogenic plasma is calculated based upon a 1D model using Langmuir probe measurements of electron temperature and ion-flux as boundary conditions at the targets. Such a background plasma model is described as an onion skin model (OSM) [11,12], and is a mixture of both experiment and theory. For this paper the Ohmic pulse 35430 under high recycling conditions at 16 s was simulated. In the SOL an allowance has been made for full heat convection, that is both thermal and kinetic, and the electron and ion temperatures have been allowed to evolve separately. Hydrogenic ionization and excitation have been included which results in some electron cooling and some impurity radiation has also been assumed to give electron temperature and density gradients which match the experimental data. Pressure (static and kinetic: $P_T = nkT(1 + M^2)$) changes throughout the SOL increasing away from the target due to charge-exchange momentum losses.

The private plasma has been treated separately from the SOL. For each inner to outer target field line, length $2L$, the electron and ion temperatures were linearly increased to a maximum of twice their target values at a distance of $L/2$ from the inner/outer target whilst the density was kept constant at its target value. Further onwards up to the stagnation point, distance L, the electron and ion temperatures remained at the maximum value whilst the density was linearly increased to twice its target value. This prescription satisfied the stagnation point:target pressure ratio of 1:2 predicted by the two-point model [9].

4.2. Diagnostic simulations

Neutral helium was injected into the private plasma at a temperature of 0.07 eV and at an angle of $+10°$ from the Z-axis. The neutral particles had a cosine distribution, with a divergence of 40° FWHM. The helium atoms travel through the divertor plasma in straight lines in the direction of their launch angle until they are ionized or collide with the divertor walls. The ionized helium is swept along the field lines out of the periscope field of view and is no longer followed. No helium recycling from the injected source or from other wall sources has been considered in this simulation. Sweeping of the separatrix has also been ignored in this example. Future simulations will account for the sweeping by running cases with the same plasma background grid and for each simulation, injecting the helium at different locations representative of the sweeping.

Each injected helium atom is followed and the excitations that each one undergoes as it moves through the plasma are calculated and registered. In this way, the neutral helium density and the density of the various helium atom excitations are calculated from the accumulated statistics of several thousand launched particles. A post-processor is then run which applies photon efficiencies from the TEXTOR atomic database [7] within ADAS [5], to which DIVIMP is coupled, at each point on the grid. The radiation intensity for each spectroscopic line of inter-

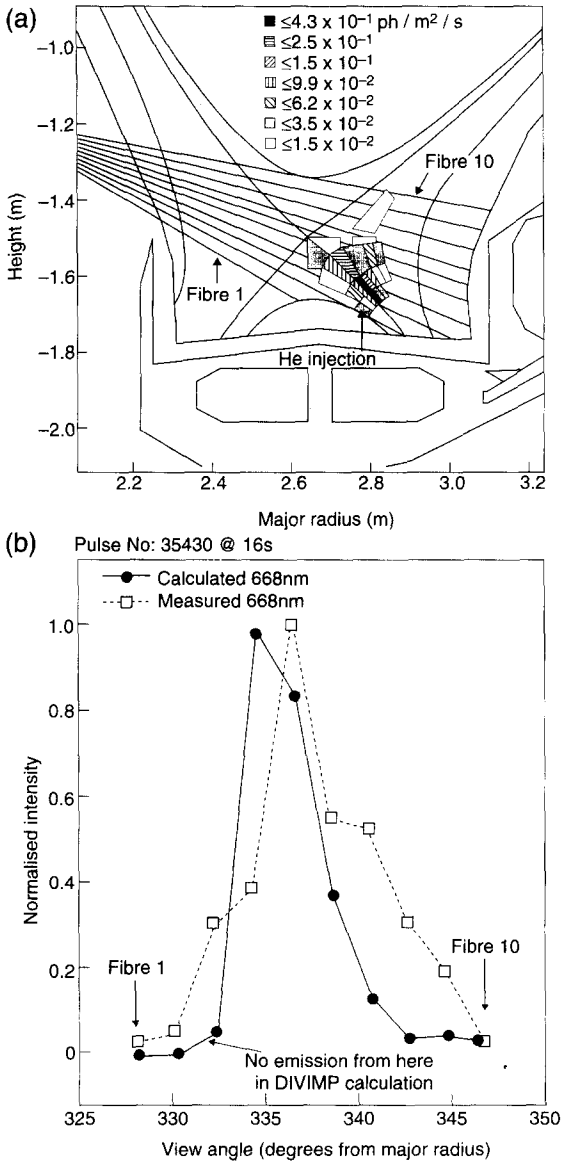

Fig. 5. (a) DIVIMP predicted spatial distribution of HeI line intensity at 728.13 nm for Ohmic pulse 35430 under high recycling conditions at 16 s and (b) normalized comparison of DIVIMP predicted and measured HeI (667.82 nm) line intensities as a function of viewing angle/fibre.

est is calculated with the assumption that the helium excited level populations are in instantaneous equilibrium with the ground level density. The experimental spectroscopic signals are simulated by integrating the calculated line intensities along the ten periscope lines of sight which also includes the effect of a finite viewing angle in the poloidal plane. A measurement of the location of these lines of sight has been obtained using the in-vessel viewing system IVIS [13]. Each line intensity is then plotted as a function of periscope viewing angle.

4.3. Results

The initial results from simulations of the helium beam diagnostic have been valuable in interpreting experimental results. The background plasma generated by the OSM gave separatrix electron temperature and density values and gradients which closely matched the experimentally determined values indicating that the HeI emission was predominantly from the separatrix. Further evidence that this was the case came from the DIVIMP calculated 2D HeI line intensity plots as shown for 728.13 nm, for example, in Fig. 5a where the peak emission is from the vicinity of the separatrix. The extent to which the DIVIMP calculated HeI line intensity as a function of periscope viewing angle matched the observed emission was also assessed as shown for 667.82 nm, for example, in Fig. 5b.

The values of the calculated density sensitive ratios (667.82 nm/728.13 nm) for each line of sight generally agree well with the corresponding experimental values as shown in Table 2. Larger variance was observed between the predicted temperature sensitive ratios (706.52 nm/728.13 nm) and the corresponding experimental values. The collisional radiative (C.R.) model of [7] used to interpret the experimental measurements presented in this paper calculated the population distributions of all energy levels up to the main quantum number $n = 4$. The upper limit in this model is determined by the ionization of helium atoms to any levels above the principal quantum number $n = 4$. The C.R. model used within ADAS to calculate the neutral helium population distributions for the DIVIMP modelling includes a strong coupling between the continuum (energy levels above $n = 4$) and the $n = 3$ and $n = 4$ populations. This difference in the population distributions calculated by the two models is more pronounced for the triplet states as the upper levels are more sensitive to this coupling, thus resulting in a large difference between the temperature sensitive line ratio, which uses the triplet line 706.52 nm, calculated from the experimental data and from ADAS. Resolving this issue is currently the main priority in the development of this interpretative model so that ADAS can be used for the interpretation of both experimental and simulated data.

Table 2
Comparison of DIVIMP calculated HeI line ratios with experimentally recorded ratios

Fibre	706.52 nm/728.13 nm		667.82 nm/728.13 nm	
	DIVIMP	measured	DIVIMP	measured
3	9.8	9.3	6.6	5.9
4	20	6.7	5.4	4.1
5	15.4	6.1	6.8	4.6
6	10	5.6	6.0	5.0
8	10	4.2	4.2	4.4

5. Concluding remarks

A thermal helium beam diagnostic has been successfully implemented in the JET MkI divertor with measurements performed in Ohmic and L-mode discharges. These measurements provide data essential for the understanding of divertor physics and for the experimental validation of detachment models such as EDGE2D. OSM calculated electron temperatures and densities are in good agreement with the helium beam measured data. Under high divertor density conditions the measured electron density probably represents a lower estimate and future work will concentrate on taking into account other atomic processes such as volume recombination which become significant at these high densities.

An interpretative model using the DIVIMP Monte Carlo code which can, for example, incorporate the helium beam divergence and periscope lines-of-sight, has been and will continue to be developed. At present there is a discrepancy in the ADAS database with respect to Ref. [7] for the triplet HeI line 706.52 nm which is currently being resolved. The DIVIMP code will also be used to investigate the effect of various recycling sources, the inclusion of electron–ion recombination from an ionized state of helium and the effect of separatrix sweeping on the helium distribution.

In the MkIIa divertor there is an additional injection point from the outer divertor side which is viewed spectroscopically from above. Other activities include the development of de Laval nozzles (see, for example, Ref. [14]) in collaboration with the Rutherford Appleton Laboratory, UK, to obtain a more collimated helium beam.

Acknowledgements

The authors would like to acknowledge P. Andrew, T. Budd, Th. Hartrampf, J. How, H. Jensen, N. Lam, P. Prior, C. Walker, C. Wilson and M. Wykes for their invaluable assistance in the implementation of the thermal helium beam diagnostic at JET following the original proposal by G.F. Matthews, G. McCracken (currently at MIT), P.D.

Morgan, B. Schweer (KfA Jülich), P.C. Stangeby and H.P. Summers.

References

[1] B. Schweer et al., J. Nucl. Mater. 196–198 (1992) 174.
[2] A. Loarte, these Proceedings, p. 118.
[3] R.D. Monk et al., these Proceedings, p. 396.
[4] P.C. Stangeby and J.D. Elder, A Guide to the DIVIMP Code (1995).
[5] H.P. Summers, JET-IR(94) 06 (1994).
[6] K. Burrell, Rev. Sci. Instrum. 49 (1978) 948.
[7] B. Brosda, Ph.D. thesis (Rühr-Universitat, Bochum, 1993).
[8] R. Reichle et al., in: Proc. 22nd EPS Conf. on Contr. Fus. Plas. Phys. 19C (1995) III-085.
[9] M. Keilhacker et al., Phys. Scr. T2(2) (1982) 443.
[10] A. Loarte et al., in preparation.
[11] S.K. Erents et al., these Proceedings, p. 433.
[12] R.D. Monk et al., J. Nucl. Mater. 220–222 (1995) 612.
[13] T. Raimondi et al., 14th SOFT, France (1986).
[14] R. Courant and K.O. Friedrichs, Supersonic Flow and Shock Waves, Vol. I (1961) chapt. V, p. 377.